Bulgarian Chemical Communications, Special Edition F, (pp. 87 – 95) 2016

Study of hydraulic performance and pressure pulsation characteristics of the grinder pump in case of clogging

X. Wang, Y. Lu*, R. Zhu, Q. Fu, W. Zhong

National Research Center of Pumps, Jiangsu University, Zhenjiang, Jiangsu 212013, China

Received February 12, 2016; Revised December 26, 2016

In order to study the variation rule of head, efficiency and the shaft power of the non-blocking submersible grinder pump, as well as the influence of the static cutter runner clogging on its pressure pulsation when the static cutter runner is clogged, this study adopts, on the basis of experiments, RNG k-Epsilon turbulence model to carry out steady and unsteady calculation about the computational domain of the grinder pump. By analyzing 28 different clogging cases of the static cutter runner, it is found that with the clogging degree of the static cutter runner increasing, the head changes in shape of a parabola, the maximum efficiency point of the grinder pump deflects to low flow point, and the high efficiency area of the pump narrows. In the low flow area, the throttling action between the dynamic cutter and static cutter is the most important factor that affects the pump characteristics variation rule, whereas, in the high flow area, the throttling action between the dynamic cutter and static cutter, the clearance cavitation at the radial clearance, and the vortex-type cavitation on the edge of the impeller outlet together affect the pump characteristics variation rule of the submersible grinder pump; inside of the submersible grinder pump, when the static cutter runner is clog-free or part of the runner is not completely clogged, the passing frequency of the dynamic cutter is the most important factor that affects the pressure pulsation, whereas, when part of the static cutter runner is completely clogged, the dynamic-static interaction effect between the dynamic cutter and static cutter is the most important factor that affects the pressure pulsation.

Key words: Submersible Grinder Pump, turbulence model, Channel blockage, pressure pulsation, cavitation.

INTRODUCTION

With the rapid development of industry and agriculture, more and more sewage thus generated contains fiber and other impurities, ordinary sewage pump is prone to be clogged during the run time so that it is unable to meet the requirement of discharging substance with high fiber impurities, as a result, sewage pump with auxiliary cutting or grinding device is more and more widely used. Therefore, the submersible grinder pump is widely used in industries such as municipal, sewage treatment, environmental protection, light industry, mining, study making, water conservancy and chemical industry, etc.

Scholars both at home and abroad have made a deep study into the submersible pump, among which for the first time in 1979, Kratzer A [1] systematically summarized design and model selection issues of the sewage pump, and emphatically analyzed the lossless performance of various pump when discharging materials; J.A. Escobar [2] studied safety of the submersible pump by analyzing submersible pump system breakdown caused by stress corroded fitting bolt through X-ray fluorescence spectrum; Parviz Ali-Zadea [3] carried out study on submersible pump noise, analyzed the relations between interference level and noise level and provided a noise elimination plan; Hernandez - Solis, A and Carlsson, F [4] studied the relation between submersible centrifugal pump cavitation and motor power capacity, diagnosing cavitation and impeller damage of the submersible centrifugal pump by monitoring motor power capacity and current flow; Liu, Yingyuan [5] mainly studied the cavitation flow characteristics of the rotor pump and discussed several factors affecting the cavitation, including rotation speed, pressure difference and gap size and inlet pressure; Lee, Kyoung - Hoon [6] carried out experiments on the effects of cavitation flow instability of the double-blade axial inducer and observed the internal asymmetric cavitation and cavitation phenomenon of the inducer; Cudina [7] established correlation with pump cavitation through noise spectrum generated by cavitation, so as to test the cavitation; Domestic scholars Wang Songlin [8] and Wang Yushi [9], etc. verified the feasibility of the RNG k-ε model and the transport equation cavitation model through experiment, finding that pressure pulsation intensity under cavitation condition was 2 times as much as that under non-cavitation condition, and pressure pulsation under low flow condition was about 5 times as much as that under design condition; Zhu

* To whom all correspondence should be sent:

E-mail jsuwxl@163.com

Rongsheng and Wang Zhenwei [10, 11], etc. studied the effects on the external characteristics of the non-blocking submersible grinder pump with or without grinding device and the clearance between dynamic cutter and static cutter. It can be found that few scholars both at home and abroad studied the submersible pump performance of all aspects under clogging condition.

This study carries out simulation studies on submersible grinder pump static cutter on the basis of experiment, mainly studies the head, power capacity and efficiency variation rule and internal flowing characteristics of the static cutter runner under different clogging conditions, and analyses frequency domain and time domain characteristics of the internal pressure pulsation of the pump when static cutter runner is clogged, so as to learn the internal flow characteristics of the non-blocking submersible grinder pump and to provide theory basis for the optimization design of grinder pump.

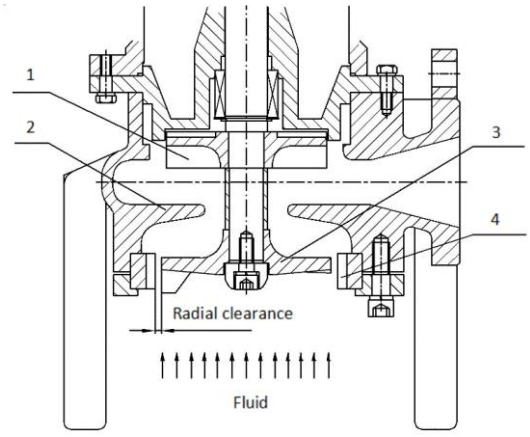

1.Pump casing 2. Impeller
3. Dynamic cutter 4.Static cutter

(a)

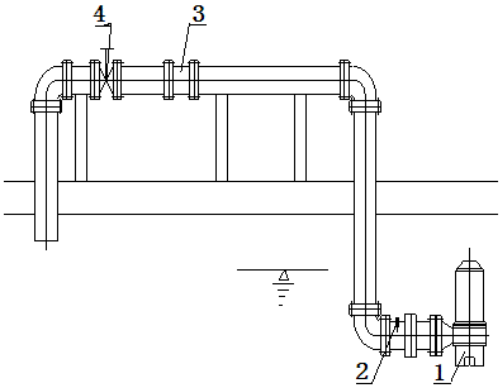

1. The Test pump 2. Piezometer tube
3.Regulating valve 4. Flowmeter

(b)

Fig. 1. Structure sketch and diagram of the test device.

NUMERICAL SIMULATION AND EXPERIMENTAL PART

Experiment table and Experiment method

Use GSP-22 non-clogging submersible grinder pump as the experimental pump, with clean water as the transmission medium. The pump performance test is carried out at the open test bed in Jiangsu University's National Water Pump and System Engineering Technology Research Center. The entire test system consists of GSP-22 non-clogging submersible grinder pump, outlet piping, comprehensive experiment table, TPA-3 pump product parameter measuring instrument, FLK1151 pressure transmitter, and NSKYLWGY liquid turbine flowmeter, etc. In order to verify the pressure pulsation characteristics of the CFD simulation, use CY301 high-precision high-speed intelligent pressure sensor to collect the pressure pulsation data at both static cutter and volute outlet. As the submersible grinder pump works underwater during the experiment, use D28 hose to provide waterproof protection to CY301, the structure sketch of pump and test device diagram, static cutter models with different partial clogging degrees and the experiment site as shown in figure 1(a),1(b), 2,3

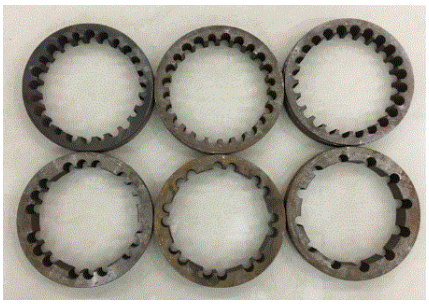

Fig. 2. Static cutter models with different partial clogging degrees

Fig. 3. Experiment site

This experiment is divided into two parts, including pump external characteristic experiment and pump pressure pulsation characteristic experiment. The pump external characteristic experiment includes 8 kinds of static cutter runner

clogging schemes with 13 flow point tests for each scheme. The experiment is started by the shutoff valve. Changing the real-time flow capacity (0 ~ 35 m3/h), the pump test system can record inlet and outlet pressure and shaft power of the centrifugal pump, and automatically calculate the head, shaft power and efficiency of the pump. Pump pressure pulsation experiment and pump external characteristic experiment are carried out simultaneously. Set the collecting zero point in the data-collecting software NetSensor before start the pump, set the sampling frequency as 2000 Hz, sampling time 30s, then collect data respectively at flow capacity points of 0.5Q, 0.7Q, 1.0Q, 1.2Q and 1.5Q.

Numerical methods

This study uses the software Pro/E to make model and adding a segment of water body in front of cutter inlet and at volute outlet, so as to guarantee higher stability of the simulation results. The entire model included water inlet, dynamic cutter water body, static cutter and rear runner water body, impeller water body, volute water body and water outlet, as shown in figure 4.

This study uses the ANSYS-CFX 14.5 to conduct numerical simulation, including steady calculation and unsteady calculation. As the static cutter of non-blocking submersible grinder pump is composed of multiple narrow half-round runner, and structured grid can take better control over the grid number than unstructured grids, and easy to converge. Therefore, use meshing software ICEM to make structured mesh division to all water body parts, and make unstructured mesh division to static cutter and rear runner water body. The grid qualities of minimum angle of each water body part are shown in Table 1.

As the grid quality directly affects the result of numerical simulation, it is only when the increase of grid number has little influence on the results that the accuracy of simulation calculation can be determined. In order to determine whether the grid number and quality of the computational domain meet the practical requirements, independence inspection on the grid of the model is carried out based on Standard k-ε and RNG k-ε turbulence models respectively. Dividing the model on the basis of different mesh density, the calculation shows that when the grid number reaches 12037.56 million, the design-point head variation range of grinder pump is below 5%, and when the grid number reaches up to 15832.73 million, the design-point head variation range of grinder pump is below 1%, indicating that the calculation results has nothing to do with the grid number. Considering the accuracy and efficiency of calculation, numbers are finally determined as follows: inlet water body grid number 334656, dynamic cutter water body grid number 1619.04 million, static cutter and rear runner water body grid number 4832.16 million, impeller water body grid number 4092 million, volute water body grid number 2100.5 million, outlet water body grid number 623.1 million, and the total model grid number 16613.36 million.

As the CFX has introduced a large number of turbulence models, it can run simulation of most of the hydraulic rotating machinery. In order to make the simulation result closer to reality, this study chooses the RANS two-equation model of Standard k-Epsilon model and RNG k-Epsilon model, the Shear Stress Transport model, the BSL model and k-Omega model. Big difference exists among the velocity distribution at different locations of the whole water domain. Calculation shows that the minimum Reynolds number at the pump inlet is and the maximum Reynolds number at the static cutter runner is , in which the Reynolds number range applies to the 5 kinds of turbulence model above.

Comparing the above 5 kinds of turbulence model simulation results (head variation curve and efficiency variation curve) and experimental data, it is found that in the low flow area (0 ~ 0.6 Q), the k-w model coincides best with the experimental data, followed by BSL > RNG k-ε > SST > Standard k-ε; around the design point (0.7 ~ 1.2 Q), the RNG k-ε model coincides best with the experimental data, followed by SST >k-w > BSL >k-ε; in the high flow area (1.2 ~ 2.0 Q), BSL model coincides best with the experimental data, followed by RNG k-ε>k-w > Standard k-ε> SST, as shown in figure 5.

Table 1. Grid quality of each part.

Grid	Water inlet	Dynamic cutter water body	Static cutter water body	Impeller	Volute	Water outlet
Quality	0.70	0.43	0.41	0.57	0.45	0.72
Min angle	48	29	23	38	33	53

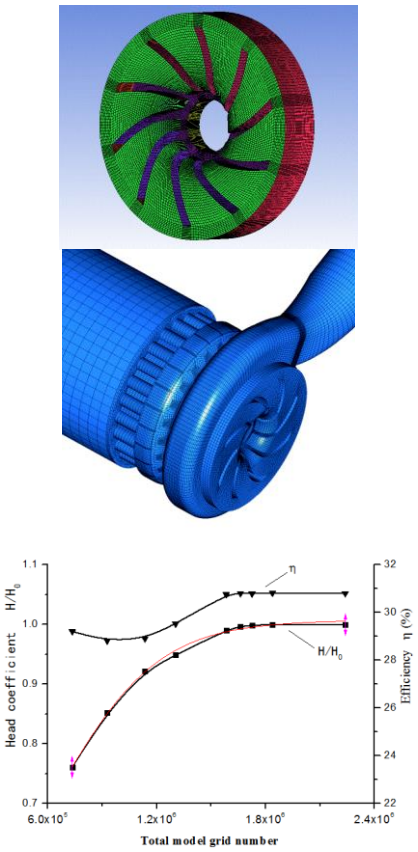

Fig. 4. Grid and grid-independent test

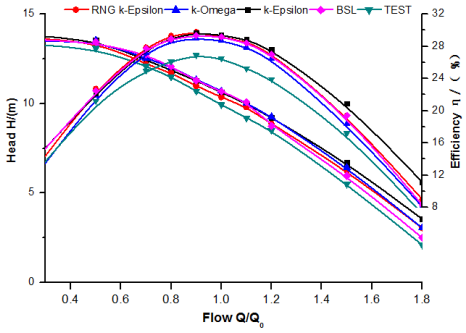

Fig. 5. Comparison of different turbulence models.

Through comprehensive analysis, the RNG k-ε model is selected as the main turbulence model of this calculation and and SIMPLE algorithm is adopted to couple pressure and velocity; based on the finite volume method of finite element to discrete equations, the dynamic and static coupling surface between impeller and volute, as well as between dynamic cutter and static cutter water body uses Frozen Rotor interface, of which the convection term of the equation uses High resolution scheme, whereas the diffusion term uses central difference scheme, with the reference pressure being1101 325 Pa.

In order to make the calculation of the flow field closer to reality, pressure inlet and quality outlet are used to set the boundary conditions during calculation. Based on submersible depth of non-clogging submersible grinder pump in actual work field, set the inlet pressure as 200 000Pa; set the wall roughness as 10μm; and use non-slip boundary conditions at the solid sidewall. Convergence scheme selects Root Mean Square Residual (RMS) of all control volumes in the computational domain, and set the convergence precision of RMS as 10^{-5}.

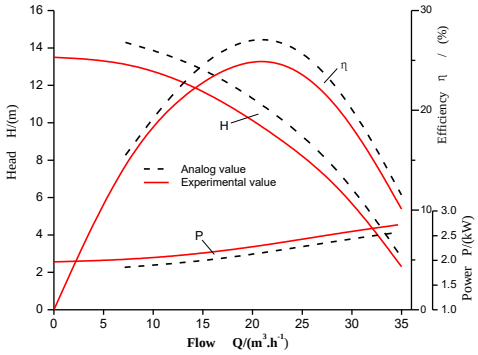

Fig. 6. Comparison of simulation prediction and experiment results.

Figure 6 shows the comparison between the experiment of the submersible grinder pump with grinding device and simulation of external characteristic curve. It can be seen that: there is certain deviation between submersible grinder pump simulation value and model machine performance experiment value, with head deviation less than 6% and efficiency deviation less than 8%. The CFD simulation calculates that the overall performance is better than the experiment performance of model machine, but the overall curve trend is consistent with better match degree. As the numerical simulation calculates only the hydraulic efficiency of fluid calculation domain and considers only the hydraulic loss of the calculation domain, whereas, except for the hydraulic loss, a lot of losses, such as leakage loss and mechanical loss, as a result, numerical simulation of the submersible grinder pump external characteristic using CFD software has certain accuracy and reliability. Whereas, the collecting data of pressure pulsation experiment verifies that the passing frequency of the dynamic cutter is the most important frequency affecting pressure pulsation when the static cutter runner is clog-free. When 1/8, 1/6, 1/4, 1/3 and 1/2 of the static cutter runner is clogged, the dynamic-static interference frequency of the dynamic and static cutter is the most important frequency that affects the pressure pulsation.

RESULTS AND DISCUSSION

Calculation model uses the GSP-22 non-clogging submersible grinder pump, with the design parameters of the model shown in table 2.

This study mainly studies the effects of the long and narrow runner blockage of grinder pump static cutter, on the hydraulic performance and pressure pulsation characteristics of grinder pump. There are two kinds of research conditions about static cutter runner clogging: research 1 studies the effect of different number of runner clogging on grinder pump external characteristics; and as part of the static cutter runners are not completely clogged, research 2 studies effects of different clogging degree on grinder pump external characteristics.

Effects of different number of grinder pump static cutter runner blockages on hydraulic performance of the grinder pump

As the grinding device runner of submersible grinder pump is both narrow and long, clogging in part of the runner often happens in actual operation. The grinding device runner number in this model is 24. In order to study the effects of clogging degree of the grinding device on grinder pump external characteristics, analog computation is carried out on pump external characteristics of water body models with different clogging number of static cutter runners. In this study, a total number of 28 static cutter water body models are set up, respectively are 3 non-clogging water body models (large runner, small runner and combination of large runner and small runner), 2 two-clogged runner water body models, 2 four-clogged runner, 3 six-clogged runner water body models, 5 eight-clogged runner water body models, 2 ten-clogged runner water body models, 5 twelve-clogged runner water body models, 2 fourteen-clogged runner water body models, 2 sixteen-clogged runner water body models, and 2 partly not completely clogged runner. Mainly analyze the effect laws of runner clogging degree on grinder pump head, efficiency and shaft power.

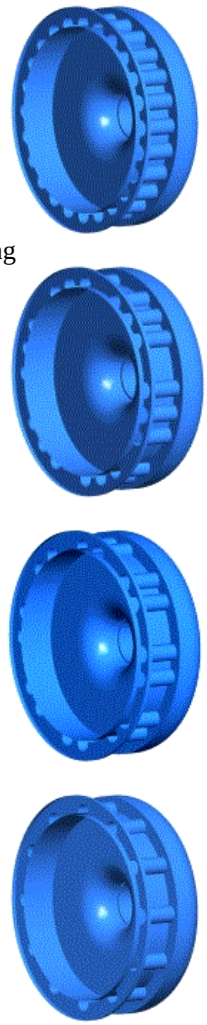

(a) non-clogging

(b)1/4 clogged

(c) 1/3 clogged

(d) 1/2 clogged

Fig. 7. Static cutter water body models with different partial clogging degrees.

Analysis of the effects of static cutter runner clogging on grinder pump head

This section mainly analyzes the effects of static cutter runner clogging degree on grinder pump head characteristics at flow capacity of 0.7Q, 1.0Q and 1.2Q, and verifies hydraulic models respectively with static cutter runner clogging degree of 0, 1/2, 1/3, 1/4 by experiments. Figure 8 shows the simulation results of head characteristics, in which it can be found that with the increase of static cutter runner clogging degree, head varies in shape of a parabola.

Table 2. Design parameters of experimental pump

Design point flow $Q/m^3 . h^{-1}$	Design point head, H/m	Rotational speed $n/r.min^{-1}$	Specific rotational speed, n_s	Impeller outside diameter, D_2/mm	Impeller outlet width, b_2/mm	Impeller hub diameter, d_h/mm	Blade outlet angle, β_2	Blade number, Z
22	10	2900	147.1	112	16	39	63	10

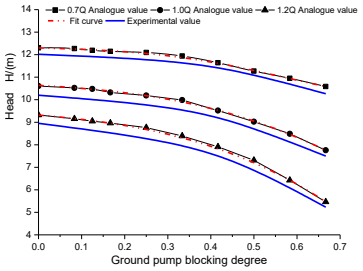

Fig.8. Effects of static cutter runner clogging on grinder pump head.

Comparison of head curves respectively at flow capacity of 0.7Q, 1.0Q and 1.2Q shows that static cutter runner clogging has greater impact on the head under high flow working condition. In order to study effect laws of static cutter runner clogging degree on the head under different flow capacity conditions, linear fits the head analog data on the basis of least square method. Carry out tendency prediction comparative analysis on the data respectively by three schemes of linear regression, polynomial regression and exponential regression, of which the quadratic polynomial fitting scheme is optimal, as shown in figure 5. It can be seen in the figure that the fitting effect is quite ideal, with the black fine lines representing the analog variation curves of the grinder pump with different clogging number, the red lines representing the tendency fitting line of head variation rules, and the blue lines showing the actual experimental variation curves of head. The equations of relations between grinder pump and clogging degree variation rules of static cutter runner at flow capacity of 0.7Q, 1.0Q and1.2Q are as follows:

$$H = -3.72\left(\frac{n}{24}\right)^2 + H_{0.7Q} \quad , \quad R^2 = 0.9371,$$

$$H' = -7.44\left(\frac{n}{24}\right); \qquad (1)$$

$$H = -6.30\left(\frac{n}{24}\right)^2 + H_{1.0Q} \quad , \quad R^2 = 0.9689,$$

$$H' = -12.60\left(\frac{n}{24}\right); \qquad (2)$$

$$H = -8.259\left(\frac{n}{24}\right)^2 + H_{1.2Q} \quad , \quad R^2 = 0.9967,$$

$$H' = -16.52\left(\frac{n}{24}\right); \qquad (3)$$

In the equations above, $H_{0.7Q}$, $H_{1.0Q}$ and $H_{1.2Q}$ represent respectively the heads at flow capacity of 0.7Q, 1.0Q and1.2Q under non-clogging static cutter runner condition, R2 represents the variance of simulation data corresponding to the head fitting equation. The head variation rule equation H' shows that the effect of grinder pump static cutter clogging on pump head at flow capacity of 1.2Q is 2.5 times as much as the effect at flow capacity of 0.7Q. On the one hand, it is because as flow capacity increases, flow velocity at the clearance increases, the contraction and diffusion loss at the clearance increases significantly, the throttling action of dynamic and static cutter radial clearance becomes more obvious, and the throttling action of radial clearance is not obvious with a correspondingly reduced hydraulic loss because of the small flow velocity under low flow working condition. On the other hand, it is because as the flow velocity of the fluid between dynamic cutter and static cutter increases, pressure drops caused by clearance cavitation and more serious cavitation. The static cutter runner clogging degree is in direct proportion to flow area of the dynamic and static cutter. Combined with the head variation rule equation H, the pump head variation is in direct proportion to the square of dynamic and static cutter flow area, that is, the throttling action at the clearance is in direct proportion to the square of the fluid flow velocity. Whereas, without grinding device, the flow area at the pump inlet has little impact on pump head, with no obvious regularity.

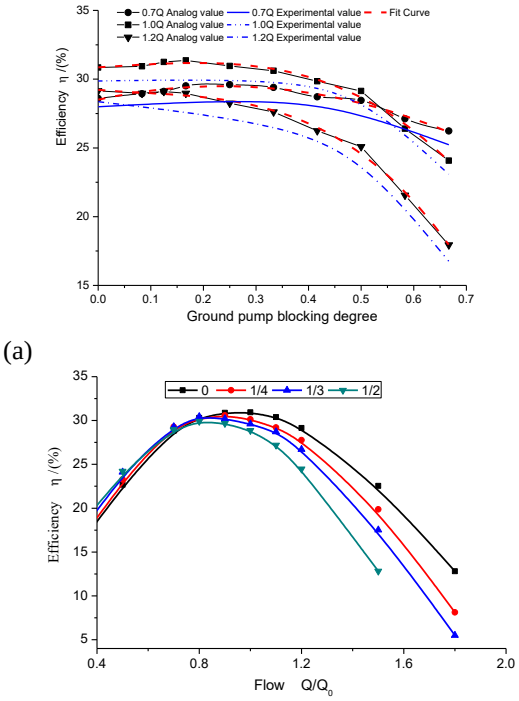

Fig. 9. Effects of static cutter runner clogging on grinder pump efficiency.

Analysis of the effects of static cutter runner clogging on grinder pump efficiency

Figure 9 (a) is the effect curve of static cutter runner clogging degree on grinder pump efficiency characteristics, with the black fine lines representing the analog variation curves of the

grinder pump efficiency, the blue lines representing the actual experimental variation curves of efficiency, and the red lines representing the tendency fitting lines of efficiency variation rules. It can be found that the variation tendencies of efficiency curve at flow capacity of 0.7Q, 1.0Q and1.2Q are completely different. When flow capacity is 0.7 Q, the efficiency curve of grinder pump shows a tendency of ascending firstly then descending with the static cutter runner clogging degree, with grinder pump efficiency being 28.6% under non-clogging condition and pump efficiency being 26.23% when clogging degree reaching 2/3.

It is thus clear that the static cutter clogging has little impact on pump efficiency at low flow capacity point. When the flow capacity is 1.0 Q, partial clogging (with clogging degree under 0.4) of the static cutter runner has little impact on pump efficiency, then decreases significantly. When clogging degree exceeds 0.55, the pump efficiency is lower than the efficiency at flow capacity of 0.7 Q under the same working condition. When flow capacity is 1.2Q, the efficiency curve of grinder pump descends significantly with static cutter runner clogging degree, especially when clogging degree exceeds 1/2. Combined with figure 9 (b), it can be seen that the maximum efficiency point of the grinder pump shifts to low flow capacity point and the high efficiency area of the pump narrows with the variation of the static cutter runner clogging degree of the grinder pump. This is mainly because that under high flow working condition, fluid flow velocity increases, pressure decreases, serious cavitation intensifies the static cutter runner clogging, as a result, the performance of the submersible grinder pump at high flow area is seriously affected by runner clogging.

To sum up, as the static cutter runner clogging degree varies, the throttling action between dynamic cutter and static cutter at low flow area is the most important factor affecting the pump characteristics variation rule, whereas, the throttling action between dynamic cutter and static cutter, clearance cavitation at the radial clearance as well as the vortex-type cavitation at the impeller outlet at high flow area together affect the pump characteristics variation rule of the submersible grinder pump.

Study on the effect of static cutter runner clogging degree on the pressure pulsation characteristics of submersible grinder pump

As the static cutter runner clogging degree increases, more unstable factors appear inside the submersible grinder pump, such as the existence of eddy current and reflux of fluid at the static cutter affected by cavitation, vortex inside the bladeless cavity, and pressure pulsation of high strength and high frequency caused by the collapse of cavitation bubbles, etc. Through the analysis of pressure pulsation frequency domain, factors that affect the unstable flow inside the pump can be found by the relations between pressure pulsation intensity and frequency. As a result, this section mainly analyzes the pressure pulsation frequency domain of the submersible grinder pump. In order to monitor the variation rule of pressure, respectively set up 8 pressure monitoring points evenly along the peripheral direction at the half-round runner outlet of the static cutter and 4 at the wall of the volute outlet, take samples of the pressure data at a fixed time interval t within time T, with the sampling frequency greater than twice the highest signal frequency.

Figure 10 shows the time domain charts of pressure pulsation at the static cutter runner outlet after deducting the inlet static pressure in different clogging schemes, with the abscissa representing 2 periods of rotation and ordinate representing the pressure intensity P. It can be observed from figure 12(a), 12(b), 12(c) and 12(d) that the period of waveform variation rule of time domain is 0.5T. Each period has 12 small fluctuations under non-clogging and partly not completely clogged conditions, 4 large fluctuations and 4 small fluctuations with 1/3 clogged, and 6 large fluctuations with 1/2 clogged. Sequence diagram periodic fluctuation is mainly caused by the rotation of the two-blade dynamic cutter, whereas, small fluctuations in the period is caused by the dynamic-static interaction effect between the dynamic cutter and static cutter, and the range of small fluctuation increases with the increase of clogging degree becoming the main component of the pulse. With the increase of flow capacity, pressure at the static cutter runner outlet drop significantly, pulsation amplitude increases significantly. At flow capacity of 0.7Q, the maximum pulsation amplitudes with 1/3 and 1/2 of the static cutter runner clogged are 17706 Pa and 23018 Pa, respectively as 1.20 times and 1.56 times of the pulsation amplitudes under non-blocking condition.

Figure 11 is the pressure pulsation frequency domain characteristic diagram at the static cutter runner outlet under different clogging degrees of the grinder pump static cutter runner. In this model, amplitudes and frequency-domain characteristics at different monitoring points under different working conditions of grinder pump are obtained through

fast Fourier transform of monitoring point pressures, with the rotational speed of grinder pump n = 2900 r. min^{-1}. As a result, the rotation frequency of the impeller is f_0 = 48.33 Hz, the dynamic cutter blade number is 2, impeller blade number is 10, tooth passing frequency f = 2 f_0 = 96.66 Hz, and blade passing frequency f = 10 f_0 = 483.33 Hz. By observing figure 11 (a), 11 (b) and 11 (c), it can be found that the pressure pulsation frequencies are distributed at 96.66 Hz (2 f_0) and at multiples of this frequency. Figure 11 (a) representing non-clogging static cutter runner and figure 11(b) representing partly not completely clogged runner, the maximum pulsation amplitude in both figures are at the frequency of 193.33 Hz (4 f_0), and the pulsation amplitude at the frequency of 1160 Hz (24 f_0) is obviously higher than the amplitude of adjacent harmonic frequency. Figure 11 (c) and 11 (d) representing conditions of 1/3 and 1/2 clogged static cutter runner, the maximum pulsation amplitudes of the two figures are respectively at the frequency of 386.66 Hz (8 f_0) and 580 Hz (f_0), with the maximum pulsation amplitude about 1.74 times as much as that of the non-clogging static cutter runner, and the second largest pulsation amplitude at the frequency of 193.33 Hz (4 f_0), with the pulsation amplitude close to that of non-clogging static cutter runner.

Figure 12 is the pressure pulsation at the volute outlet in different clogging schemes. It can be seen that under both non-clogging and partly not completely clogged conditions, the maximum pulsation amplitude at the volute outlet is the passing frequency of the dynamic cutter and the second largest pulsation amplitude is the passing frequency of the impeller blade. When 1/3 and 1/2 static cutter runner is clogged, the maximum pulsation amplitudes of both conditions are at the dynamic-static interference frequency, and the second largest pulsation amplitude frequency is the passing frequency of the impeller blade. The above analysis shows that inside of the entire submersible grinder pump, when the static cutter runner is clog-free or partly not completely clogged, the passing frequency of the dynamic cutter is the most important factor affecting the pressure pulsation; when part of the static cutter runner is completely cogged, the dynamic-static interaction effect of the dynamic and static cutter is the most important factor affecting the pressure pulsation and being verified in the pressure pulsation experiment.

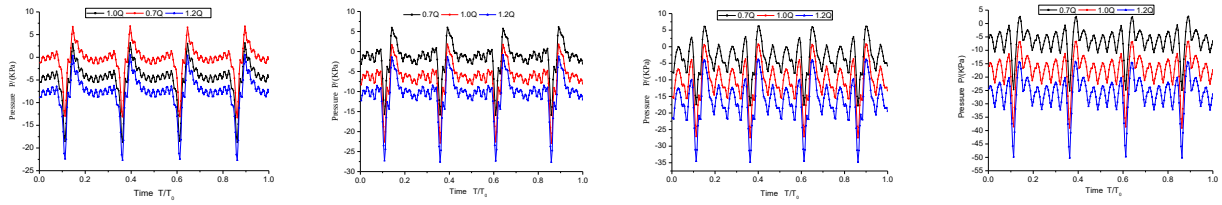

(a) non-clogging (b) partly not completely clogged (c) 1/3 clogged (d) 1/2 clogged

Fig. 10. Time domain diagram of pressure fluctuation at the static cutter runner.

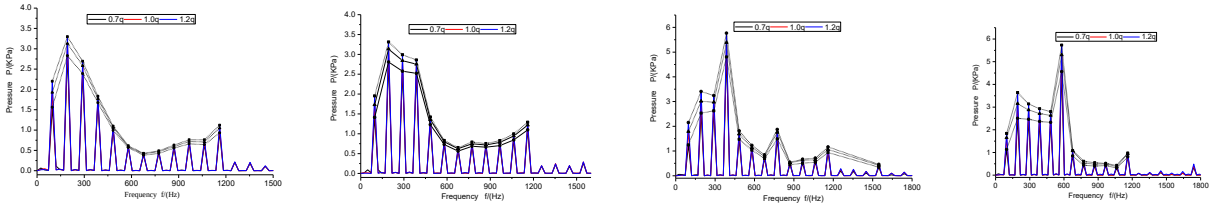

(a) non-clogging (b) partly not completely clogged (c) 1/3 clogged (d) 1/2 clogged

Fig. 11. Frequency domain diagram of pressure fluctuation at the static cutter runner

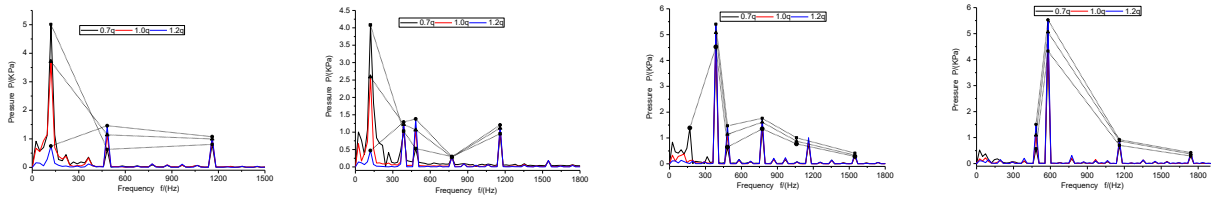

(a) non-clogging (b) partly not completely clogged (c) 1/3 clogged (d) 1/2 clogged

Fig. 12. Frequency domain diagram of pressure fluctuation at the volute outlet.

CONCLUSIONS

(1) By the 28 established static cutter water body models with different clogging degrees, it is found that as the static cutter runner clogging degree increases, the head declines in shape of a parabola, the maximum efficiency point of the grinder pump shifts to low flow capacity point, and the high efficiency area of the pump narrows. The throttling action between dynamic cutter and static cutter at low flow area is the most important factor affecting the pump characteristics variation rule, whereas, the throttling action between dynamic cutter and static cutter, clearance cavitation at the radial clearance as well as the vortex-type cavitation at the impeller outlet at high flow area together affect the pump characteristics variation rule of the submersible grinder pump.

(2) Through analysis of the time domain and frequency domain of inlet and outlet pressure pulsation of the submersible grinder pump in different clogging schemes, it can be found that in the submersible grinder pump, when the static cutter runner is clog-free or partly not completely clogged, the passing frequency of the dynamic cutter is the most important factor affecting the pressure pulsation; when part of the static cutter runner is completely cogged, the dynamic-static interaction effect of the dynamic and static cutter is the most important factor affecting the pressure pulsation.

Acknowledgments: *This research was financially supported by: (1)National Natural Science Foundation of China (51379091); (2)A science and technology program funded by Natural Science Foundation of Jiangsu Province (BK20130516); (3)National Youth Natural Science Foundation of China (51509112); (4) Key R & D programs of Jiangsu Province of China (BE2015129 AND BE2016160); (5)Prospective joint research project of Jiangsu Province(BY2016072-02); (6)Supported by the Open Research Fund of Key Laboratory of ministry (provincial),（Xihua University）, szjj2016-070; (7)Jiangsu Province ordinary university graduate student research innovation project（KYLX16_0894）*

REFERENCES

1. F. Aschenbach, *World Pumps*, **355**, *42 (1996)*.
2. J.A. Escobar, A.F. Romero, J. Lobo-Guerrero, *Engineering Failure Analysis*, **60**, 1 (2015).
3. P. Ali-Zadea, C. Hajiyevb, U. Hajiyevac, M. Yilmazd, *Journal of Petroleum Science and Engineering*, **110**, 109 (2013).
4. A. Hernandez-Solis, F. Carlsson, *European Power Electronics and Drives*, **20**(1), 58 (2010).
5. L. Yingyuan; W. Leqin; Z. Zuchao. *Journal of Mechanical Engineering Science*, **229**(14), 2626 (2015).
6. L. Kyoung-Hoon; Y. Joo-Hyung; K. Shin-Hyoung. *Journal of Mechanical Science And Technology*, **23**(9), 2350 (2009).
7. M. Cudina,; J. Prezelj, *Applied Acoustics*, 22(4), 540 (2009).
8. W. Songlin, T. Lei, W. Yuchuang, *Journal of Vibration and Shock*, **32**(22), 168 (2013).
9. W. Yuchuang, T. Lei, C. Shuliang, Z. Baoshan, *Journal of Mechanical Engineering*, **50**(10), 163 (2014).
10. Z. Rongsheng, W. Zhenwei, L. Peng, W. Xiuli, *Journal of agricultural mechanization research*, **5**, 179 (2013).
11. Z. Weiguo, L. Ming, L. Yi, S. Jianping, S. Qice. *Journal of Drainage and Irrigation Machinery Engineering*, **12**, 1033 (2015).